13th Australasian Fluid Mechanics Conference
Monash University, Melbourne, Australia
13-18 December 1998

BALL FALLING THROUGH VISCOPLASTIC FLUID IN A CYLINDER

Li Chen[1], J. A. Reizes[2], E. Leonardi[3] and Yuguo Li[1]
1. Division of Building, Construction and Engineering, CSIRO
PO Box 56, Highett, Vic. 3190
2. School of Mechanical Engineering
University of Technology Sydney, PO Box 123, Broadway NSW 2007
3. School of Mechanical and Manufacturing Engineering
University of New South Wales, Sydney 2052

ABSTRACT
A numerical method for a spherical ball falling through a Bingham fluid in a cylinder is presented in this paper. The singularity of the Bingham model is omitted by adopting an exponential constitutive equation. An explicit location of the yielded surface is no longer required in the entire solution procedure. This study has two main motivations: first, to develop a numerical model for the transient flow of suspensions in slurry in a complex geometry with the inertia effect; and second, to seek solutions of the stress contribution and to identify any yielded surface for this flow. It is confirmed that a yielded fluid cavity gradually develops around the ball, and its size decreases with an increase in yield stress. The diameter of a torus of fluid in almost rigid-body rotation in the cavity increases with an increase in yield stress. There is no visible attachment of unyielded fluid on the front stagnation point of the ball, however a small amount of fluid with very small stress does exist in this region. No solid attachment is observed at the rear stagnation point.

INTRODUCTION
The settling of suspended particles in Bingham liquids is of interest from many fundamental aspects. It also represents an important group of industrial phenomena. For example, the detergent industries have the problem of suspending abrasive particles in mobile liquid detergents. The oil industries need to suspend propane in fracturing fluid, and mineral industries require transporting of slurries. An important feature of Bingham fluids is a yield stress which must be exceeded before significant deformation can occur.

Although extensive research has been carried out on obtaining the solution for Bingham fluids in lubrication flow, they mainly concern a steady state creeping flow in a simple geometry (e.g. O'Donovan and Tanner 1984, Gartling and Phan-Thien 1984, Wilson and Taylor, 1996). Limited studies can be found for the flow of a Bingham fluid in a complex geometry. A major difficulty in numerical and analytic procedures is determining the location of the yielded surface. Indeed, there is a dispute in the literature about the possibility of the existence of an unyielded flow region in a complex geometry (e.g. Lipscombe and Denn 1984); Sherwood and Durban 1996). Beris *et al.* (1985) obtained results for the creeping motion of a ball in Bingham fluids, and their results show the existence of an unyielded region in this complex geometry. Walton and Bittleston (1991) and Beverly and Tanner (1992) studied the axial flow of a Bingham fluid in a narrow eccentric annulus. Both demonstrated the existence of an unyielded or plug region.

In this paper, we also study the problem of a spherical ball falling through a Bingham fluid in a cylinder using a robust numerical method. The flow is transient and not inertia free.

MATHEMATICAL FORMULATION
Consider an initially stationary metal ball in a cylinder filled with a Bingham fluid, as shown in Figure 1.

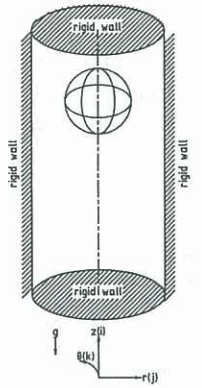

Figure 1: A Schematic Description of the Problem

The ball moves downwards due to gravity, and the shear forces within the Bingham liquid are gradually established so that part of the fluid may be yielded, which will flow. The rest will behave as a solid: the so-called unyielded region. The non-dimensional variables are given by:

$$p^* = \frac{p}{p_{ref}}, \mathbf{U}^* = \frac{\mathbf{U}}{u_{ref}}, \mathbf{x}^* = \frac{\mathbf{x}}{R_0}, \quad t = \frac{t}{t_{ref}}, \rho^* = \frac{\rho}{\rho_f}, \mu^* = \frac{\mu}{\mu_f}, \tag{1}$$

where

$$u_{ref} = \sqrt{gR_0}, \; p_{ref} = \rho_f u_{ref}^2 . \tag{2}$$

Navier-Stokes equations are applied to the whole domain contained interfaces with the surface tension force effect, and can be written in a non-dimensional form as:

$$\nabla \bullet \mathbf{U} = 0 , \tag{3}$$

$$\frac{\partial(\rho \mathbf{U})}{\partial t}+\nabla \bullet(\rho \mathbf{U} \otimes \mathbf{U})=-\nabla p+ \frac{1}{\mathrm{Re}} \nabla \bullet \underline{\underline{\tau}}+\rho \mathbf{g}+\frac{1}{\mathrm{Bo}} \sigma \kappa \delta(\mathbf{x}-\mathbf{x}_i) \hat{\mathbf{n}}, \quad (4)$$

where

$$\underline{\underline{\tau}}=\mu(\dot{\gamma}) \underline{\underline{\dot{\gamma}}}, \quad (5)$$

$$\rho(\mathbf{x}, t)=F(\mathbf{x}, t) \rho_f+[1-F(\mathbf{x}, t)] \rho_s, \quad (6)$$

$$\mu(\mathbf{x}, t)=F(\mathbf{x}, t) \mu_f+[1-F(\mathbf{x}, t)] \mu_s. \quad (7)$$

$\mathbf{U}(\mathbf{x}, t)=(u_r, u_\theta, u_z)$ is the fluid velocity; $\mathbf{x}(r, \theta, z)$ is the position; ρ is the density; μ is a generalised Newtonian viscosity, which is a function of the second invariant of the strain-rate described in the following text; p is the pressure; $\mathbf{g}$ is the gravitational acceleration vector; and $\underline{\underline{\dot{\gamma}}}$ is the strain-rate tensor. The subscripts f and s denote liquid and solid phase respectively, and i denotes an interface. Reynolds number and Bond number are defined by $\mathrm{Re}=\frac{\rho_f g^{1/2} R_0^{3/2}}{\mu_f}$, $\mathrm{Bo}=\frac{\rho_f g R_0^2}{\sigma}$. F, the volume fraction occupied by the liquid which lies between 0 and 1, is used as an indicator of the interface. It is governed by:

$$\frac{\partial F}{\partial t}+\nabla \bullet(\mathbf{U} F)=0. \quad (8)$$

The last term of equation (4) is the surface tension force, in which σ is surface tension, δ is the delta function, $\hat{\mathbf{n}}$ is the unit normal of an interface, and κ is local curvature, and are given by:

$$\hat{\mathbf{n}}=\nabla F / |\nabla F|, \quad \kappa=-(\nabla \cdot \hat{\mathbf{n}}). \quad (9)$$

The surface tension force is modelled by the continuum surface tension force (CSF) developed by Brackbill *et al* (1992).

The non-dimensional Bingham model, with the reference variables defined in Equation (1), can be rewritten as:

$$\begin{aligned} \underline{\underline{\tau}} &= -\left(1+\frac{We}{\dot{\gamma}}\right) \underline{\underline{\dot{\gamma}}} \quad \tau \geq \tau_y \\ \underline{\underline{\dot{\gamma}}} &= 0 \quad \tau < \tau_y \end{aligned} \quad (10)$$

where

$$\tau=\pm \sqrt{\frac{1}{2}\left(\underline{\underline{\tau}}:\underline{\underline{\tau}}\right)} \text{ and } \dot{\gamma}=\pm \sqrt{\frac{1}{2}\left(\underline{\underline{\dot{\gamma}}}:\underline{\underline{\dot{\gamma}}}\right)} \quad (11)$$

The Weisenberg number is defined by $We=\frac{2 \tau_y R_0}{\mu_f u_{ref}}$.

It is noted that the ideal Bingham model (Eq. 10) requires a prior knowledge of the position of a yield surface, which distinguishes the "solid" and "fluid" regions. However, this immediately introduces a numerical difficulty because of the singularity of this model at $\dot{\gamma}=0$. In order to overcome the difficulty, a variety of modifications have be made, such as that by Beris *et al.* (1985) who introduced a "regularisation" parameter into the constitutive equation (10) and obtained a converged solution on the basis of the continuous decrease of this parameter. They presented excellent results for creep motion of a sphere in a Bingham fluid, but their method involved a large number of unknowns. In their model, the yielded surface is defined by a critical second invariant of the strain rate tensor $\dot{\gamma}_c$, which is a function of the drag coefficient and the Weisenberg number (We). Gartling and Phan-Thien (1984) suggested a bi-viscosity model, in which the material behaves as a highly viscous liquid, with viscosity μ_r at very low shear rates τ_r, and a transition in behaviour, named yielding, occurs above a critical second invariant of the strain-rate tensor, $\dot{\gamma}_c$. After yielding, the fluid holds on the apparent viscosity, $\mu_0+\frac{\tau_y}{\dot{\gamma}}$. This model was adopted by Beverly and Tanner (1992). In this model, it is no longer necessary to distinguish computationally between an absolute rigidity region ($\dot{\gamma}=0$) and sheared region ($\dot{\gamma}>0$). Therefore the difficulty in dealing with the discontinuity of equation (10) no longer exists. The yield point in terms of the second invariant of the strain-rate tensor is set by the fluid yield stress, τ_y and a specified high viscosity, μ_r. However, the bi-viscosity model cannot be reduced to the Bingham model when $\dot{\gamma}=0$.

Papanastasiou (1987) suggested an exponential constitutive equation:

$$\underline{\underline{\tau}}=-\left(1+\frac{We[1-\exp(-h\dot{\gamma})]}{\dot{\gamma}}\right) \underline{\underline{\dot{\gamma}}}, \quad (12)$$

in which h is an exponential growth parameter. This exponential relation suggests that a yield stress can be established even at a very small strain rate by means of a material parameter that controls an exponential development of stress. This model holds continuously in yielded and unyielded regions. Thus the singularity of equation (10) is omitted. With a large h, the model (Eq.12) approximates the ideal Bingham liquid (Eq.10) well. A smooth transition from a state of infinitely high viscosity to one of yielding can be secured by an appropriate selection of the exponential growth parameter. However, a question about where the interface is between the unyielded and yielded regions may still be raised due to this smoothness. In this study, a yielded surface is determined by:

$$\frac{\tau_c}{We}=\left(\frac{\dot{\gamma}_c}{We}+[1-\exp(-h\dot{\gamma}_c)]\right)=1, \quad (13)$$

and h = 150 is used in all simulations. With this parameter, $\dot{\gamma}_c = 0.0312$ for We = 4.0 and $\dot{\gamma}_c = 0.0334$ for We = 6.0.

In all cases discussed in this paper, a spherical ball is initially located on the axis of a closed cylinder filled with a stationary fluid.

NUMERICAL METHOD

The control volume method is used to discretise the PDEs on a collocated grid. The SIMPLE method is adopted for the velocity-pressure coupling. The motion of the ball is tracked by the modified VOF algorithm (Chen *et al.*1996).

No *a priori* knowledge about the location of the ball is required. The motion of the ball is coupled with the whole solution procedure. Therefore the complex moving boundary problem is converted to the challenge of an interface tracking.

A backward differencing scheme was used for the time derivative term and the standard central differencing is adopted for the diffusion terms. For the convection term, a second-order upwind-based scheme is used. The details of the implementation of the numerical method can be found in Chen and Li (1998).

RESULTS AND DISCUSSIONS

The numerical method was developed based on the original code for the study of the rise of gas bubbles in viscous liquids. The validations of the code and the mesh sensitivity study have been reported in Chen *et al.* (1996). The ball motion in this study is much slower than the rise of a gas bubble, therefore the mesh size used for the study of gas bubble rising is considered to be fine enough to produce accurate results for this study.

In order to observe flow characteristics of a ball falling in Bingham fluids, a ball falling in a Newtonian fluid is also simulated. A significantly different behaviour for the Newtonian and Bingham fluids is observed.

The vertical velocity contours at $t = 4.5$ for the Newtonian and Bingham fluids are shown in Figure 2 with Re = 100, Bo = 50 and $\rho_f/\rho_s = 0.25$. In order to illustrate the different flow behaviour, displayed velocities were related to the corresponding ball-falling velocities in this figure. It can been seen that this relative velocity becomes constant away from the ball with a distance approximately equal to the diameter of the ball when $We = 6$, and this distance increases with a decrease in We. This means that for Bingham fluids, the fluid beyond this distance is undisturbed. For the Newtonian fluid ($We = 0$), the fluid was moving in a much larger region, and such flow region was decreased with an increase in We. However, the attachment of solid-type fluid at the front and rear stagnation points of the ball can not be identified from this figure.

The relative vertical velocity profile in the radial direction at a plane across the centre of the ball is shown in Figure 3. The velocity profile becomes flatter when the yield stress of fluid is higher. A torus plug starts to form when $We \neq 0$.

For the Newtonian fluid, since equation 13 was not applicable, the second invariant of strain rate is shown in Figure 4. In this figure, the contour levels show at a range of 0 to 0.2. The normalised second invariant of stress rate are shown in Figures 5 and 6 for Bingham fluids. The yielded surface is indicated by a contour level with a value of 1 in these figures. There is a significant difference in fluid flow fields between the Newtonian and Bingham fluids. For the Newtonian fluid, the deformation of the fluid is significant as time progresses, which is illustrated by the development of contours with values larger than 0 (Figure 4). However, for the Bingham fluids, when We = 4, the fluid in a small cavity surrounding the falling ball is yielded where contour values are higher than 1, indicating deformations of the fluid existed (see Figure 5). The fluid outside the cavity behaves as a solid. As the yielded cavity is establishing, and a torus of fluid in almost rigid-body rotation gradually forms inside the cavity, where the value of the second invariant of stress rate is close to 1. As Beris *et al.* (1985) stated, the fluid particles in the torus rotate as a rigid-body and translate in the direction of ball falling due to a higher shear rate near the ball. It should be noted that the torus was not centred at the symmetry plane of the ball as predicted by Beris *et al.* (1985). This may be caused by inertia and wall effects. When We increases further from 4 to 6, the volume of the cavity decreases (Figure 6) and the torus becomes larger, which is consistent with that predicted by Beris *et al.* (1985). This fluid cavity moves with the falling ball with a nearly fixed shape and volume. The unyielded fluid outside the cavity behaves as a solid.

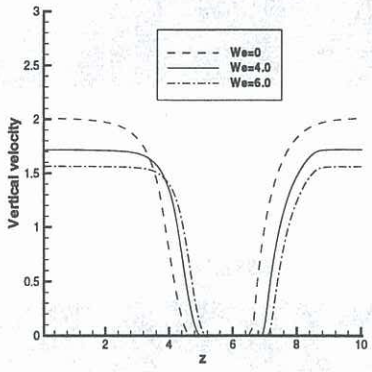

Figure 2: Effect of yield stress on relative vertical velocity profiles along the z-axis (Re = 100, Bo = 50, $\rho_f/\rho_s = 0.25$)

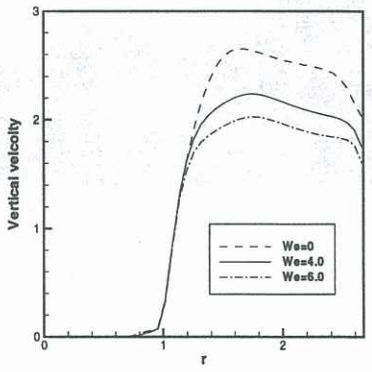

Figure 3: Effect of yield stress on vertical velocity distribution at the cross-section of the centre of the ball (Re = 100, Bo = 50, $\rho_f/\rho_s = 0.25$)

When We = 4, there is a slightly larger volume attached to the front stagnation point of the ball, where the value of the normalised second invariant of stress rate is very close to 1, compared with that when We = 0. With an increase in We from 4 to 6, this volume becomes larger. Although a yielded surface with a value of normalised second invariant of strain rate exactly equal to 1 can not be identified with the yield stresses used in this study, a very small solid cap could be expected if a much finer grid or a very high yield stress was used. This will be our future study. According to

Beris *et al.* (1985), the maximum height of their solid cap is less than 8% of the ball radius. There is no attachment of solid on the rear stagnation point of the ball during the simulations. This may result from the inertial and wall effects.

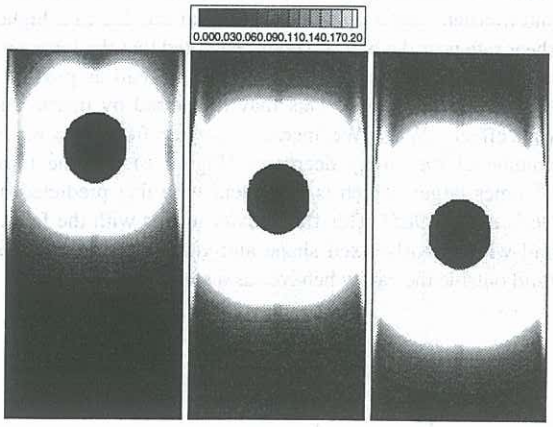

Figure 4: Contours of the second invariant of the strain rate tensor at We = 0 (Re = 100, Bo = 50, $\rho_f/\rho_s = 0.25$)

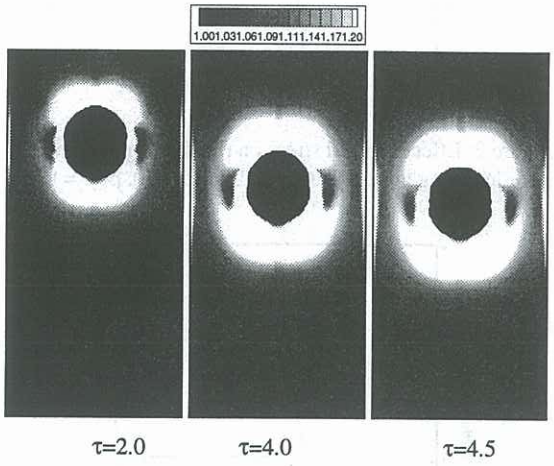

Figure 5: Contours of the normalised second invariant of the strain-rate tensor for We = 4 (Re = 100, Bo = 50, $\rho_f/\rho_s = 0.25$)

CONCLUSION

A numerical method for a ball falling in Bingham fluids has been presented in this paper. An exponential constitutive equation has been used to model the yield stress of Bingham fluids. There is no prior knowledge of the locations of yielded and ball interfaces required for the simulation. It has been found that for Bingham fluids, only the fluid in a cavity is significantly deformed. The volume of the cavity decreases with an increase in yield stress, and it will travel with the ball in a fixed shape. No solid attachment is found in the rear stagnation point of the ball, however, a very small cap of very small fluid deformations is observed on the front stagnation point of the ball. The cap will grow with an increase in yield stress.

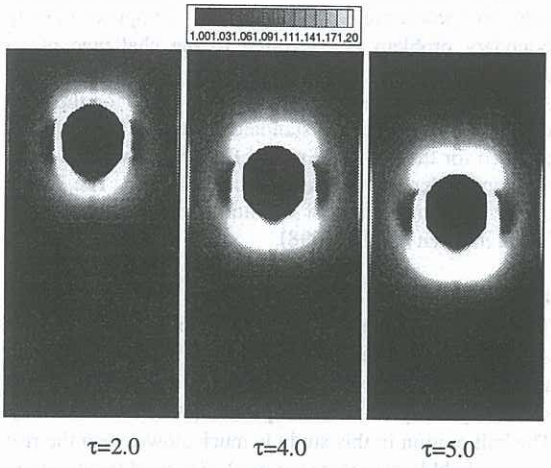

Figure 6: Contours of the normalised second invariant of the strain-rate tensor for We = 6 (Re = 100, Bo = 50, $\rho_f/\rho_s = 0.25$)

REFERENCE

BERIS A.N., TSAMOPOULOS, J.A., RAMSTRONG, R.C. and BROWN, R. A, "Creeping motion of a sphere through a Bingham fluid", *J. Fluid Mech,*. **158**, 219-244, 1985.

BEVERLY, C.R. and TANNER, R.I., "Numerical analysis of three-dimensional Bingahm plastic flow", *J. Non-Newtonian Fluid Mech.,* **42**, 85-115, 1992.

BRACKBILL, J.U., KOTHE, D.B. and ZEMACH, C., "A continuum method for modeling surface tension," *J. Comp. Phys.*, **100**, 335-354, 1992.

CHEN, L., GARIMELLA, S.V., REIZES, J.A., and LEONARDI, E., "Analysis of bubble rise using the VOF Method: I Isolated bubbles", *ASME Proceedings of the 31st NHT Conference*, Houston, **4**, 161-173, 1996.

CHEN, L. and LI, Y., "A numerical method for two-phase flows with an interface", *Environmental Modelling & Software* (in press), 1998.

GARTLING, D.K. and PHAN-THIEN, N., "A numerical simulation of a plastic fluid in a parallel-plate plastometer", *J. Non-Newtonian Fluid Mech..*, **14,** 347-360, 1984.

LIPSCOMBE, G.G. and DENN, M.M., "Flow of Bingham fluids in complex geometries", *J. Non-Newtonian Fluid Mech.*, **14**, 337-408, 1984.

O'DONOVAN, E.J. and TANNER, R.I., "Numerical study of the Bingham squeeze film problem", *J. Non-Newtonian Fluid Mech.*, **15,** 75-83, 1984.

PAPANASTASIOU, T.C., "Flow of material with yield", *J. Rheology*, **31**(5), 385-404, 1987.

SHERWOOD, J.D. and DURBAN, D., "Squeeze flow of a power-lay viscoplastic solid", *J. Non-Newtonian Fluid Mech.*, **62,** 35-54, 1996.

WALTON, I.C. and BITTLESTON, S.H., "The axial flow of a Bingham plastic in a narrow eccentric annulus", *J. Fluid Mech.* **222**, 39-60,1991.

WILSON, S.D.R. and TAYLOR, A.J., "The channel entry problem for a yield stress fluid", *J. Non-Newtonian Fluid Mech.*, **65,** 165-176, 1996.